This is the accepted manuscript made available via CHORUS. The article has been published as:

Optimizing electrically controlled echo sequences for the exchange-only qubit

Niklas Rohling and Guido Burkard

Phys. Rev. B **93**, 205434 — Published 24 May 2016

DOI: 10.1103/PhysRevB.93.205434

Optimizing electrically controlled echo sequences for the exchange-only qubit

Niklas Rohling* and Guido Burkard
Department of Physics, University of Konstanz, D-78457 Konstanz, Germany

Recently, West and Fong [New J. Phys. **14**, 083002 (2012)] introduced an echo scheme for an exchange-only qubit, which relies entirely on the exchange-interaction. Here, we compare two different exchange-based sequences and two optimization strategies, Uhrig dynamical decoupling (UDD) and optimized filter function dynamical decoupling (OFDD), which were introduced for a single-spin qubit and are applied in this paper to the three-spin exchange-only qubit. The calculation shows that the adaption of the optimization concepts can be achieved by straight-forward calculation. We consider two types of noise spectra, Lorentzian and Ohmic noise. For both spectra, the results reveal a slight dependence of the performance on the choice of the echo sequence.

I. INTRODUCTION

The concept of exchange-only quantum computation [1] relies on all-electrical qubit control. Exchange-only qubits are defined as two-dimensional subspaces of three electron spins. Given the advantages of all-electrical control of these qubits, it is important to investigate the possible decoherence mechanisms and their mitigation using appropriate techniques. While a homogeneous magnetic field of unknown strength does not harm the qubit state, an inhomogeneous magnetic field, which might occur due to nuclear spins in the host material, can cause decoherence and leakage. In the case of the resonant-exchange qubit [2, 3], the degeneracy of the qubit (and leakage) states is partially lifted by the always-on exchange coupling. In an external magnetic field, the leakage can be suppressed completely and dephasing may be corrected by an echo sequence resembling the single-spin qubit spin echo[4]. For the degenerate exchange-only qubit, the situation is more complicated due to the existence of a leakage state [5]. Applying spin-echo techniques to each spin individually is not favorable as this requires magnetic control which contradicts the concept of exchange-only quantum computing [4]. West and Fong [6] introduced an echo scheme for the exchange-only qubit which is based on SWAP operations between neighboring spin states. These operations are provided directly by the exchange interaction. The basic idea is to average the acquired phases of the spin states by permuting their positions within the triple quantum dot. A sequence which also corrects erroneous SWAP gates was introduced by Hickman *et al.* [7].

In this paper, we focus on optimization strategies for the timing of the pulses in exchange-based echo schemes. We assume that the pulse lengths are negligible and the decoherence occurs between the pulses. West and Fong [6] already applied Uhrig dynamical decoupling (UDD) [8, 9] to their SWAP-based sequence for the exchange-only qubit. Here, we transfer the concept of the optimized filter function dynamical decoupling (OFDD) [10] from the single-spin to the three-spin system. Furthermore, we consider two different SWAP sequences and compare their performance for a simple Carr-Purcell-Meiboom-Gill (CPMG) timing of the pulse as well as for UDD and OFDD.

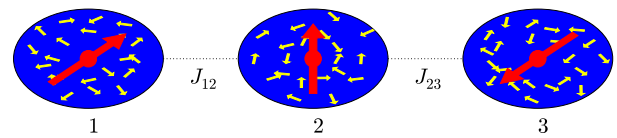

FIG. 1. (Color online) Sketch of the system of three quantum dots each hosting an electron represented by a large red (gray) dot and arrow. The electron spin states in dots 1 and 2 (2 and 3) can be coupled via the exchange interaction J_{12} (J_{23}), while there is no direct coupling between dots 1 and 3. The electron spins in each dot experience the influence of the nuclear spins, which are represented by small yellow (light gray) arrows, via the hyperfine coupling. We describe this influence of the nuclear spins by fluctuating Overhauser fields.

The paper is organized as follows. In Sec. II, a model for the system of interest is introduced. Sec. III contains the calculation to obtain the fidelity in dependence of the pulse sequence and the noise spectrum. In Sec. IV the optimization strategies for the timing of the pulses are discussed and the results for the fidelity compared to the unchanged qubit are presented. Finally, we conclude in Sec. V.

II. EXCHANGE-ONLY QUBIT IN A RANDOM MAGNETIC FIELD

The system which we consider here consists of three quantum dots hosting one electron spin each, see Fig. 1. The electron spins are coupled by the exchange interaction and influenced by local magnetic fields,

$$H = \frac{J_{12}}{4}\boldsymbol{\sigma}_1 \cdot \boldsymbol{\sigma}_2 + \frac{J_{23}}{4}\boldsymbol{\sigma}_2 \cdot \boldsymbol{\sigma}_3 + \sum_{i=1}^{3} \mathbf{B}_i \cdot \boldsymbol{\sigma}_i \qquad (1)$$

* present address: Department of Physics, Norwegian University of Science and Technology, NO-7491, Trondheim, Norway

where the exchange couplings J_{12} and J_{23} can be electrically controlled [11, 12]. Here, $\boldsymbol{\sigma}_i = (\sigma_{ix}, \sigma_{iy}, \sigma_{iz})^T$ denotes the vector of Pauli operators for the spins in dots $i = 1, 2, 3$. The magnetic field $\mathbf{B}_i = B_{\text{ext}}\mathbf{e}_z + \mathbf{B}_i^O$ consists of an external magnetic field B_{ext} in z direction and the Overhauser field as a classical model for the interaction with the nuclear spin bath. In the case $B_{\text{ext}} \gg |\mathbf{B}_i^O|$, the dephasing is dominated by the z component of the Overhauser field under the condition that it is time independent, see Appendix A. This still holds for the Overhauser field changing slowly in time compared to the Larmor precession caused by B_{ext} within a rotating wave approximation [13]. In the following we consider only the magnetic field in z direction. Thus, states with different total spin in z direction will not be coupled. The qubit subspace of the exchange-only qubit is the two-dimensional space characterized by the total spin $s = 1/2$ and the spin in quantization (z) direction $s_z = 1/2$, see [1]. Therefore, leakage is possible to the state with $s = 3/2$ and $s_z = 1/2$ in the presence of a magnetic field gradient in z-direction [4]. In this work we assume that the exchange coupling is only switched of for the negligibly short time of an echo pulse and the dephasing in the Overhauser field happens for $J_{12} = J_{23} = 0$. Dephasing in the presence of a nonzero exchange coupling have been considered by Ladd [14].

III. ECHO SEQUENCES

West and Fong [6] introduced an echo scheme relying only on the exchange interaction in agreement with the concept of the exchange-only qubit. They suggested to interchange the spin information of neighboring dots in such a way that any spin state spends equal time in each of the three dots. The operations which are needed are SWAP gates for the dots 1 and 2 and for the dots 2 and 3, SWAP_{12} and SWAP_{23}. These operations are provided directly by the exchange coupling. It is assumed that this coupling can be tuned to values much larger than the differences in the Zeeman splitting between the dots. In this case, the exchange coupling is not disturbed by the Overhauser field and the gate times can be negligibly short. West and Fong considered sequences using the gates $P = \text{SWAP}_{23}\text{SWAP}_{12}$ and $P^{-1} = \text{SWAP}_{12}\text{SWAP}_{23}$ in alternating pairs, $P \to P \to P^{-1} \to P^{-1} \to P \to P \to P^{-1} \to P^{-1}$ and so on. They showed that the concept of UDD [8, 9] removing the influence of the noise up to mth order in time ($m = 0, 1, 2, 3, \ldots$) can be applied to this three-spin problem. In the present paper, we compare the sequence of alternating pairs of P and P^{-1} to the sequence using only the cyclic permutation of the spin states, P. Furthermore, we additionally use the concept of optimized noise filtration [10]. Both, OFDD and UDD, were originally introduced for a single qubit dephasing without leakage states.

We now consider the $s_z = +1/2$ subspace, starting from the product basis $\{|\uparrow\uparrow\downarrow\rangle, |\uparrow\downarrow\uparrow\rangle, |\downarrow\uparrow\uparrow\rangle\}$. In this basis the term in the Hamiltonian describing the effect of a time-dependent magnetic field in z direction is diagonal. The corresponding time evolution for the states $|\uparrow\uparrow\downarrow\rangle$, $|\uparrow\downarrow\uparrow\rangle$, and $|\downarrow\uparrow\uparrow\rangle$ evokes the phase factors, $e^{-i(\phi_1+\phi_2-\phi_3)}$, $e^{-i(\phi_1-\phi_2+\phi_3)}$, and $e^{-i(-\phi_1+\phi_2+\phi_3)}$, respectively. Formally, we track the spin state when a SWAP gate transfers it to another quantum dot. The time evolution at time T for the spin state which is in the first dot at time $t = 0$ is

$$U_1(T) = e^{-i\phi_1\tilde{\sigma}_{1z}} \text{ with } \phi_1 = \int_0^T dt\, h_1(t), \tag{2}$$

where $\tilde{\sigma}_{1z}$ is the Pauli matrix for the individual spin state labeled here with 1 although the state is stored in dots 2 and 3 for some time. This spin state experiences the magnetic field $h_1(t)$, which is the field in the dot where the spin state is stored at time t. For the spin states initially stored in the dots 2 and 3, the time evolution is given in full analogy by $U_2(T)$ and $U_3(T)$. We use the states

$$|\pm\rangle = \frac{|\uparrow\uparrow\downarrow\rangle + e^{\pm i2\pi/3}\,|\uparrow\downarrow\uparrow\rangle + e^{\mp i2\pi/3}\,|\downarrow\uparrow\uparrow\rangle}{\sqrt{3}} \tag{3}$$

as an orthogonal basis of the qubit subspace. In the corresponding Bloch sphere, with the poles $|\pm\rangle$, the eigenstates of the exchange interactions between neighboring dots lie in the equatorial plane. Therefore, SWAP_{23} and SWAP_{12} interchange $|+\rangle$ and $|-\rangle$, i.e., $\text{SWAP}_{12}\,|\pm\rangle = |\mp\rangle$ and $\text{SWAP}_{23}\,|\pm\rangle = e^{\pm i2\pi/3}\,|\mp\rangle$. Thus P and P^{-1} change only the phase when applied to the states $|+\rangle$ and $|-\rangle$, $P\,|\pm\rangle = e^{\mp i2\pi/3}|\pm\rangle$ and $P^{-1}\,|\pm\rangle = e^{\pm i2\pi/3}|\pm\rangle$. If the initial quantum state is a superposition of $|+\rangle$ and $|-\rangle$, the different phase factors can lead to a different state at the end of the sequence. In the following we will assume that those changes are reversed at the end of the sequence by applying further exchange pulses. The only relevant leakage state is

$$|L\rangle = \frac{|\uparrow\uparrow\downarrow\rangle + |\uparrow\downarrow\uparrow\rangle + |\downarrow\uparrow\uparrow\rangle}{\sqrt{3}} \tag{4}$$

with the quantum numbers $s = 3/2$ and $s_z = 1/2$. In the basis $\{|+\rangle, |-\rangle, |L\rangle\}$ the time evolution is represented by the matrix

$$U(T) = \frac{1}{3}\begin{pmatrix} e^{i\varphi_3}+e^{i\varphi_2}+e^{i\varphi_1} & e^{i\varphi_3}+e^{i(\varphi_2+\frac{2\pi}{3})}+e^{i(\varphi_1-\frac{2\pi}{3})} & e^{i\varphi_3}+e^{i(\varphi_2-\frac{2\pi}{3})}+e^{i(\varphi_1+\frac{2\pi}{3})} \\ e^{i\varphi_3}+e^{i(\varphi_2-\frac{2\pi}{3})}+e^{i(\varphi_1+\frac{2\pi}{3})} & e^{i\varphi_3}+e^{i\varphi_2}+e^{i\varphi_1} & e^{i\varphi_3}+e^{i(\varphi_2+\frac{2\pi}{3})}+e^{i(\varphi_1-\frac{2\pi}{3})} \\ e^{i\varphi_3}+e^{i(\varphi_2+\frac{2\pi}{3})}+e^{i(\varphi_1-\frac{2\pi}{3})} & e^{i\varphi_3}+e^{i(\varphi_2-\frac{2\pi}{3})}+e^{i(\varphi_1+\frac{2\pi}{3})} & e^{i\varphi_3}+e^{i\varphi_2}+e^{i\varphi_1} \end{pmatrix} \tag{5}$$

with $\varphi_j = 2\phi_j - \phi_1 - \phi_2 - \phi_3$. In this matrix, we denote the upper left 2×2 block, which describes the dynamics within the qubit subspace, by $U_Q(T)$. We compare this operation with the perfect storage of the qubit, $U_Q(T) = \mathbb{1}$. In this context, T denotes the desired storage time of the qubit. The fidelity of the time evolution with respect to the identity operation is [15]

$$F = \frac{\mathrm{Tr}(U_Q^\dagger U_Q) + |\,\mathrm{Tr}(U_Q)|^2}{6}. \tag{6}$$

Note that U_Q is not unitary. From Eq. (5), we obtain

$$F = \frac{4}{9} + \frac{5}{27}\sum_{i<j}\cos(2[\phi_i - \phi_j]) \tag{7}$$

We assume that the Overhauser fields can be described by a Gaussian distribution. Then the same holds for the acquired phases, thus we obtain

$$\langle\cos(2[\phi_i - \phi_j])\rangle = e^{-2\langle(\phi_i-\phi_j)^2\rangle}, \tag{8}$$

in analogy with the case of a single spin [9]. In order to calculate $\langle(\phi_1-\phi_2)^2\rangle$, West and Fong [6] introduced the functions $f_j(t)$, $j = 1,2,3$, which are defined according to the position of the spin states: For the initial positions, (1,2,3), where the numbers 1, 2, and 3 are the labels of the spin states, the values of the functions are $\{f_1, f_2, f_3\} = \{1, -1, 0\}$. For the positions (2,3,1), the functions are $\{f_1, f_2, f_3\} = \{-1, 0, 1\}$ and for the positions (3,2,1), they are $\{f_1, f_2, f_3\} = \{0, 1, -1\}$. The Overhauser fields are labeled according to the quantum dot where they can be found by $B_j(t)$ for dot number j, see Eq. (1). Then the phase difference between two spin states at time T is given by [6]

$$\begin{aligned}\phi_1(T)-\phi_2(T) &= \int_0^T dt\,[h_1(t) - h_2(t)] \\ &= \int_0^T dt\,[f_1(t)B_1(t)+f_2(t)B_2(t)+f_3(t)B_3(t)].\end{aligned} \tag{9}$$

The expressions for $\phi_2 - \phi_3$ and $\phi_3 - \phi_1$ can be obtained by permuting the indices of the functions $f_j(t)$. The variance is

$$\begin{aligned}&\langle(\phi_1(T) - \phi_2(T))^2\rangle \\ &= \Bigg\langle \int_0^T dt_1\,[f_1(t_1)B_1(t_1)+f_2(t_1)B_2(t_1)+f_3(t_1)B_3(t_1)] \\ &\quad\times \int_0^T dt_2\,[f_1(t_2)B_1(t_2)+f_2(t_2)B_2(t_2)+f_3(t_2)B_3(t_2)]\Bigg\rangle \\ &= \sum_{i,j\in\{1,2,3\}}\int_0^T dt_1\int_0^T dt_2 f_i(t_1)f_j(t_2)\langle B_i(t_1)B_j(t_2)\rangle \\ &= \frac{1}{\pi}\sum_{i,j\in\{1,2,3\}}\int_0^\infty d\omega\, y_i(\omega T)y_j^*(\omega T)\frac{p_{ij}(\omega)}{\omega^2}\end{aligned} \tag{10}$$

with $y_j(\omega T) := \frac{\omega}{i}\int_0^T dt\, e^{i\omega t} f_j(t)$ being, up to the factor of ω/i, the Fourier transform of the switching function $f_j(t)$, $j = 1,2,3$. The function $p_{ij}(\omega)$ is the power spectrum of $\langle B_i(t)B_j(0)\rangle$, $p_{ij}(\omega) = 2\int_0^\infty dt\,\cos(\omega t)\langle B_i(t)B_j(0)\rangle$. Under the assumption that the Overhauser fields in the dots have the same variance and the same power spectrum while being independent of each other, $p_{ij}(\omega) = \delta_{ij}p(\omega)$, the variance of the phase differences can be written as

$$\begin{aligned}&\langle(\phi_1(T) - \phi_2(T))^2\rangle \\ &= \langle(\phi_2(T) - \phi_3(T))^2\rangle \\ &= \langle(\phi_3(T) - \phi_1(T))^2\rangle \\ &= \frac{1}{\pi}\int_0^\infty d\omega\,\underbrace{[|y_1(\omega T)|^2 + |y_2(\omega T)|^2 + |y_3(\omega T)|^2]}_{=F_F(\omega T)}\frac{p(\omega)}{\omega^2}.\end{aligned} \tag{11}$$

Here $F_F(\omega T)$ is the filter function of the SWAP-based echo sequence which determines the values of $f_j(t)$ at times $t \in (0, T)$. The assumption that the Overhauser fields are described by the same random distribution also lead to a further simplification of the expression Eq. (7) for the fidelity, which assumes the form

$$F = \frac{4}{9} + \frac{5}{9}e^{-2\langle(\phi_1-\phi_2)^2\rangle}. \tag{12}$$

The value for $\langle(\phi_1 - \phi_2)^2\rangle$ will depend on the noise spectrum $p(\omega)$, the pulse sequence, and the time T. Here we focus on Ohmic noise,

$$p_{\mathrm{Ohm}}(\omega) = \omega\Theta(\omega_1 - \omega), \tag{13}$$

with a cutoff described by the Heaviside function $\Theta(\cdot)$, and Lorentzian noise,

$$p_{\rm Lorentz}(\omega) = \frac{\omega_1}{1+(\frac{\omega}{\omega_1})^2}. \tag{14}$$

The latter has been used for a model to explain experiments with a nuclear spin bath [16]. In the situation considered in this paper, the random field is also assumed to originate from the nuclear spins. Nevertheless, we perform the calculations for the Ohmic noise spectrum as well to demonstrate that the method can be applied to different noise spectra. Note that the parameter ω_1 is a sharp cutoff in Eq. (13) while it is a parameter determining the width of the spectrum in Eq. (14). Here we are interested in the scaling behavior of the fidelity with respect to the parameter ω_1. Therefore, it is possible to set the relative noise strength to one, see Ref. [10]. The generalization to an arbitrary noise strength is straightforward. As done by Uys *et al.* in Ref. [10] we express the integral in Eq. (11) by using the dimensionless variables $T' = T\omega_1$ and $\omega' = \omega/\omega_1$. Then the variance of the phase difference reads

$$\langle(\phi_1-\phi_2)^2\rangle = \int_0^\infty d\omega'\, F_F(\omega' T')\frac{\tilde{p}(\omega')}{\omega'^2}, \tag{15}$$

where the noise spectrum is rescaled,

$$\tilde{p}(\omega') = \tilde{p}_{\rm Ohm}(\omega') = \omega'\Theta(1-\omega') \tag{16}$$

or

$$\tilde{p}(\omega') = \tilde{p}_{\rm Lorentz}(\omega') = \frac{1}{1+\omega'^2}. \tag{17}$$

The filter function depends on the sequence of applied SWAP operations via the switching functions $f_j(t)$, $j = 1,2,3$. First we consider the same operation $P = \mathrm{SWAP}_{23}\mathrm{SWAP}_{12}$ applied at the times $T\delta_j$, $j = 1,\ldots,n$. Then the switching functions are periodic with respect to the time intervals $[\delta_j,\delta_{j+1})$ with period three. The switching functions f_1 and f_2 at time t are given by

$$\{f_1,f_2\} = \begin{cases} \{1,-1\} & \text{if } t/T\in[\delta_j,\delta_{j+1}),\ j \bmod 3 = 0,\\ \{-1,0\} & \text{if } t/T\in[\delta_j,\delta_{j+1}),\ j \bmod 3 = 1,\\ \{0,1\} & \text{if } t/T\in[\delta_j,\delta_{j+1}),\ j \bmod 3 = 2.\end{cases} \tag{18}$$

The third function is always determined by $f_3(t) = -(f_1(t)+f_2(t))$. For convenience, $\delta_0 = 0$ and $\delta_{n+1} = 1$ have been introduced. For the sequence with alternating pairs of P and P^{-1}, which was considered in Ref. [6], the switching functions at time t are

$$\{f_1,f_2\} = \begin{cases} \{1,-1\} & \text{if } t/T\in[\delta_j,\delta_{j+1}),\ j \bmod 4{=}0,\\ \{-1,0\} & \text{if } t/T\in[\delta_j,\delta_{j+1}),\ j \bmod 4{=}1\,\text{or}\,3,\\ \{0,1\} & \text{if } t/T\in[\delta_j,\delta_{j+1}),\ j \bmod 4{=}2,\end{cases} \tag{19}$$

and again $f_3(t) = -(f_1(t)+f_2(t))$. We compare the results for the exchange based SWAP sequences to individual spin echoes, where a σ_x gate is applied on each spin at times $\delta_j T$, $j = 1,\ldots,n$. This single spin manipulation is not compatible with the concept of exchange-only quantum computing as it requires single-spin manipulation with a time-dependent local magnetic field. It is considered here for comparison of the efficiency of the echo sequences only. In the notation used here, the switching functions for the single-spin operations are $f_1(t) = (-1)^j$ if $t/T\in[\delta_j,\delta_{j+1})$, $f_2(t) = -f_1(t)$, and $f_3(t) = 0$. For more details on the computation of the fidelities see Appendix B.

IV. WAITING TIME OPTIMIZATION STRATEGIES

In this section we apply different concepts for optimizing $\{\delta_1,\ldots,\delta_n\}$. These concepts have been introduced for single-spin echoes but can be applied for the three spin system as well. The calculation of the filter function is straight forward for a given sequence and $\langle(\phi_1-\phi_2)^2\rangle$ can be calculated with Eq. (15) by solving the respective integrals.

A. CPMG sequence

The CPMG sequence [17, 18] is defined by $\delta_1 = 1/(2n)$, $\delta_j = \delta_{j-1} + 1/n$ for $j = 2,\ldots,n$. The waiting times t_w between consecutive pulses are always the same. The waiting time between initialization and the first pulse equals the waiting time between the last pulse and the measurement at time T and is half as long as t_w. We do not expect this timing to be ideal for the exchange-based echos because it does not necessarily lead to a situation where each spin state spends the same time in each quantum dot during the storage time, i.e., in general, y_1, y_2, and y_3 do not vanish in first order. Nevertheless, we include CPMG timed pulses here for comparison with UDD and OFDD timing, see below. The infidelity $1-F$ for the CPMG timing is presented in Fig. 2. The fidelity F can be increased with an increasing number of pulses. Applying the echo sequences is more effective for the Ohmic noise, which is stronger at higher frequencies compared to the Lorentzian noise. Note that the better scaling behavior of the infidelity in Fig. 2 for the all cyclic sequence and $n = 3$ ($P\to P\to P$) originates from the fact that y_j ($j = 1,2,3$) vanishes up to first order for this sequence if n is an integer multiple of 3. But for larger values of T', the sequences with $n = 4$ and $n = 10$ can have more significant larger effect on the fidelity than $n = 3$.

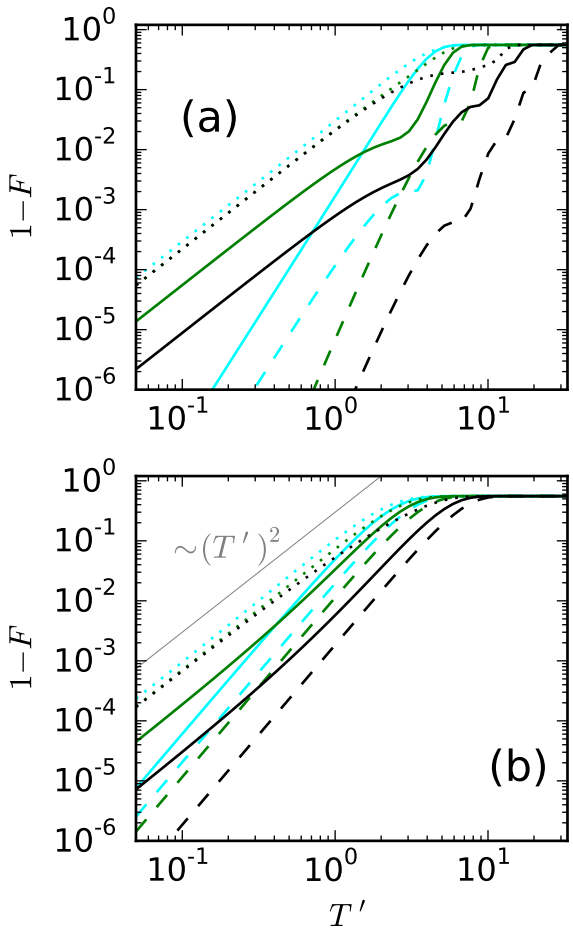

FIG. 2. (Color online) Infidelity $1-F$ for Ohmic noise (a) and Lorentzian noise (b) in dependence of dimensionless storage time T' for pulse times chosen according to the CPMG scheme. The number of applied pulses n are $n = 3$ (cyan, light gray), $n = 4$ (green, dark gray), and $n = 10$ (black). The applied sequences are the all-cyclic permutations realized by applying $P = \mathrm{SWAP}_{12}\mathrm{SWAP}_{23}$ at every time $T\delta_j$ (solid lines), the sequence of pairs of P and P^{-1} (dotted lines) and the single spin operations (dashed lines).

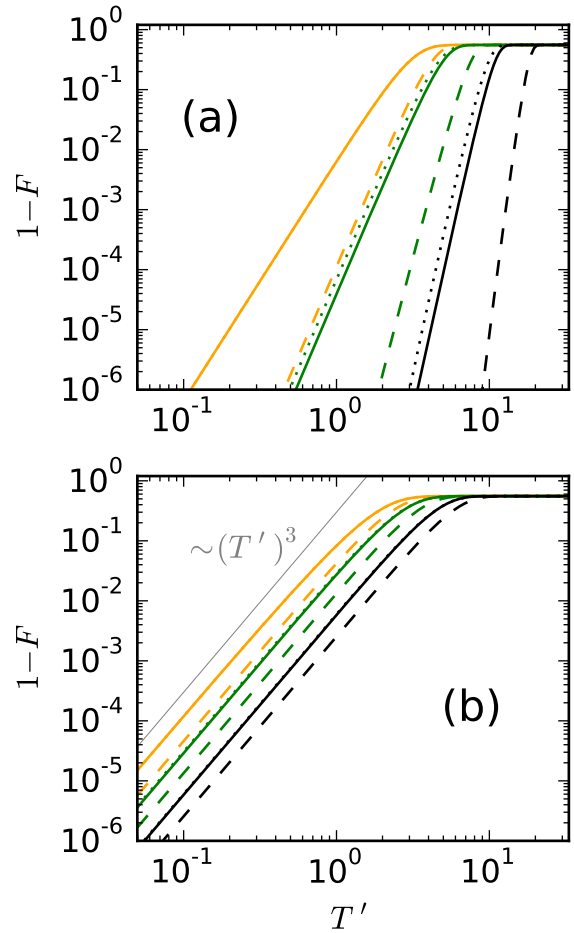

FIG. 3. (Color online) Infidelity $1-F$ in dependence of dimensionless storage time T' for Ohmic noise (a) and Lorentzian noise (b) for pulse times chosen according to the UDD optimization strategy. The number of applied pulses n are $n = 2$ (orange, light gray), $n = 4$ (green, dark gray), and $n = 10$ (black). The applied sequences are plotted in the same line styles as in Fig. 2. In (b) the results for the exchange-based pulses with the all-cyclic permutations and the pairs of P and P^{-1} are very similar, thus the solid and the dotted lines are on top of each other. For $n = 2$ these sequences are identical by definition. The better performance of the single-spin pulses (dashed lines) compared to the SWAP-based sequences for the same number of pulses, n, is due to the fact that it allows for the filter function to be zero up to the order n while it is only order $n/2$ for the SWAP-based pulse sequences.

B. Applying Uhrig-type dynamical decoupling

The concept of UDD [8, 9] requires that the functions $y_j(\omega' T')$ $(j = 1, 2, 3)$should be zero up to an order m,i.e.,

$$\left(\frac{\partial}{\partial(\omega' T')}\right)^k y_j(\omega' T')\bigg|_{\omega' T'=0} = 0, \qquad (20)$$

for $k = 0, \ldots, m$. The equation for $k = 0$ is fulfilled by the definition of y_j. If Eq. (20) is fulfilled for $j = 1$ and $j = 2$, it automatically holds for $j = 3$. Uhrig showed that the respective condition for single spin storage can be achieved by $n = m$ pulses [8]. Moreover, the values for δ_j are given by the analytical expression $\delta_j = \{1 - \cos(\pi j/[n+1])\}/2$ [8] in this single-spin case. West and Fong [6] extended this concept to the exchange-only qubit for the sequence $P \to P \to P^{-1} \to P^{-1} \ldots$. In this situation the number of pulses has to be $n = 2m$. Here, we also apply the concept to the sequence $P \to P \to P \ldots$ again with $n = 2m$. For both sequences, the sequence introduced by West and Fong and the all P sequence, one has to solve a system of $2m$ polynomial equations for $\delta_1, \ldots, \delta_{2m}$ with powers up to m. Finding these systems of equations is straightforward for the given switching functions. The values of δ_j for the P only

m	δ_j	all cyclic	West-Fong sequence
1	δ_1	$\frac{1}{3}$	$\frac{1}{3}$
2	δ_1	$\frac{3-\sqrt{5}}{6}$	$\frac{1}{6}$
	δ_2	$\frac{1}{3}$	$\frac{1}{3}$
3	δ_1	$\frac{3-\sqrt{6}}{9}$	$\frac{4-\sqrt{10}}{9}$
	δ_2	$\frac{9-\sqrt{33}}{18}$	$\frac{5-\sqrt{10}}{9}$
	δ_3	$\frac{6-\sqrt{6}}{9}$	$\frac{4}{9}$
4	δ_1	0.033987060628007174	$\frac{1}{3}-\sqrt{\frac{2}{27}}$
	δ_2	0.10778050263957079	$\frac{5}{12}-\sqrt{\frac{35}{432}}$
	δ_3	0.24541246139134222	$\frac{7}{12}-\sqrt{\frac{35}{432}}$
	δ_4	0.40712677534489696	$\frac{2}{3}-\sqrt{\frac{2}{27}}$
5	δ_1	0.0197219731840097	0.0422244245173296
	δ_2	0.0671399277438179	0.0940587956886883
	δ_3	0.1583859791807335	0.2172228408817372
	δ_4	0.27816415473255296	0.2838895075484039
	δ_5	0.42457938477024890	0.4518343711713587
6	δ_1	0.013679963095182367	0.0313685011617312
	δ_2	0.046973639574998944	0.0691609286752199
	δ_3	0.11189155743938264	0.1617103538537611
	δ_4	0.19981242938137375	0.2161866929592387
	δ_5	0.31156471269738840	0.3514848584641742
	δ_6	0.43493416837050681	0.4258827585118745
7	δ_1	0.0094699468692662485	0.0239219438795333
	δ_2	0.033350661076818913	0.0535688803938237
	δ_3	0.080564753596069461	0.1262566342290569
	δ_4	0.14684156194511558	0.1675244212375237
	δ_5	0.23329457080574879	0.2761133079137736
	δ_6	0.33333333333333333	0.3417044666375784
	δ_7	0.44366705640151921	0.4698392155798953

TABLE I. UDD-optimized pulse times for the all cyclic sequence and the West-Fong sequence from Ref. [6]. Note that the pulse times not included in the table are given by $\delta_j = 1 - \delta_{2m+1-j}$. The numerical results for West-Fong sequence ($m = 5, 6, 7$) are from Ref. [6]. The all cyclic and the West-Fong pulse times only coincide for $m > 1$ if the sequences are identical.

sequence are different from the values in the West-Fong sequence for $n > 2$. In Tabel IV B we present the values for δ_j for orders $m = n/2 = 1, \ldots, 7$. For $n = 2$ the two sequences are identical. In Fig. 3, we also present the infidelities for $n = 4$ and for $n = 10$. In general, the values of δ_j can be found numerically while a closed expression is unknown for the SWAP-based sequences, see also [6]. Comparing Fig. 3 to Fig. 2, we see that UDD can outperform the CPMG sequence where the improvement is more significant for the Ohmic noise than for the Lorentzian noise. Experimental constrains might set a lower limit to the time between two pulses. Therefore, it can be useful to consider the minimum pulse interval [19, 20], which is always $\delta_1 T$ for the sequences considered here. In Fig. 4 we consider δ_1 in dependence of the order

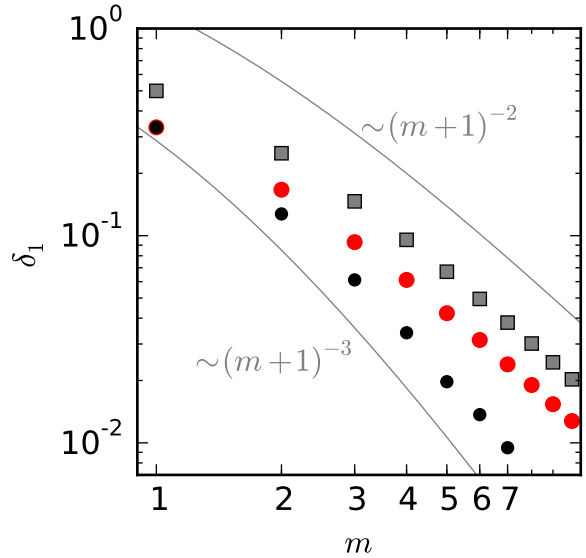

FIG. 4. (Color online) Double logarithmic plot of δ_1, which is the smallest pulse interval, in dependence of the order m for UDD applied to the all cyclic sequence (black circles), to the West-Fong sequence (red (gray) circles, values from Ref. [6]), and for comparison to a single spin problem (gray squares).

m. For the all cyclic sequence, δ_1 is always smaller than for the West-Fong sequence for $m > 1$. Furthermore, this difference becomes more significant with increasing m.

C. Applying optimized noise filtration

Another strategy for minimizing the dephasing, OFDD, was introduced by Uys *et al.* [10]. In this concept, the integral

$$\int_0^1 d\omega' \, F_F(\omega' T') \tag{21}$$

is minimized by finding a suitable set of $\{\delta_1, \ldots, \delta_n\}$. In Ref. [10] OFDD was explicitly considered for a single spin. Here we apply the method for the three-spin problem. The integrals included in (21) can be treated analytically, see Appendix B. The values of $\delta_1, \ldots, \delta_n$ have to be determined by numerical minimization of (21). As starting values for this minimization we use the CPMG values. Presumably, using UDD values as initial values would be an improvement but we included $n = 3$ where UDD values are not available and we want to use the same strategy for all n to avoid dependences of the results on details which are not essentially part of the OFDD optimization condition. The minimization program uses standard Broyden-Fletcher-Goldfarb-Shanno algorithm. If the numerical found minimum lies outside the allowed values, $\delta_j < 0$ or $\delta_j > 1$ we replace this value

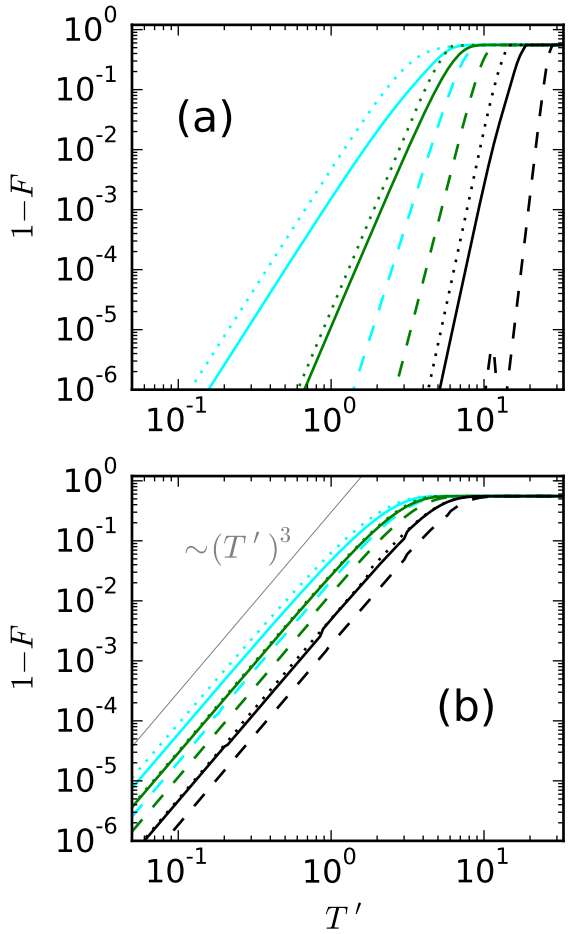

FIG. 5. (Color online) Infidelity $1-F$ in dependence of dimensionless storage time T' for Ohmic noise (a) and Lorentzian noise (b) for pulse times chosen according to OFDD. The color codes and the line styles are identical to Fig. 2.

with 0 or 1 respectively. This typically happens at large values of T' where the infidelity $1-F$ becomes large. Moreover, the found minimum is not necessarily a global minimum. This clearly happens for the single-spin echo at small T' shown in Figure 6 where the OFDD values are apart from the UDD values although we know that UDD is ideal in the limit $T' \to 0$. The results for the infidelity in dependence of the dimensionless storage time T' are shown in Fig. 5. The kink in the infidelity for the single-spin operation for $n = 10$ (black dashed line) is also a consequence of finding a non-global minimum. Despite this numerical behavior, we find that similar to the results for the single spin [10], OFDD leads to improved fidelities compared to UDD, see Fig. 7. where we compare the infidelities $1-F$ for pulse times optimezed with OFDD and UDD for $n = 10$ pulses. For all echo sequences OFDD outperformes UDD for the Ohmic noise while the results are very close to each other for the Lorentzian noise spectrum. In Fig. 6 we present the values of $\delta_1, \ldots, \delta_n$ for $n = 3, 4$ in dependence of the dimensionless storage time. The results show a symmetric behavior with respect to half of the storage time except the $n = 3$ values for the West-Fong sequence including two P and one P^{-1} pulse. Comparing the values of δ_1 in Fig. 6 (b), we see that again for the all cyclic sequence, δ_1 assumes smaller values than for the West-Fong sequence.

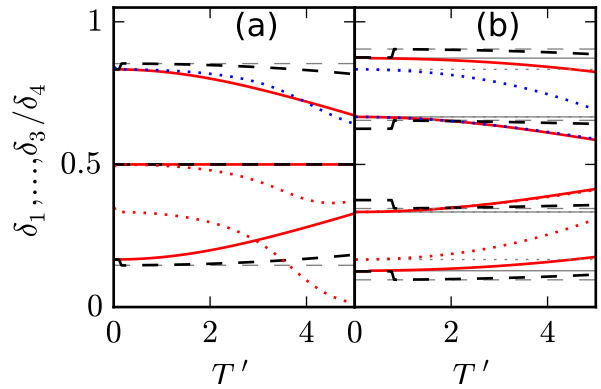

FIG. 6. (Color online) OFDD values of $\delta_1, \ldots, \delta_n$ for $n = 3$ (a) and $n = 4$ (b) in dependence of the dimensionless storage time T' considering single spin echo (black dashed lines), all cyclic operations (red solid lines), and the West-Fong sequence (dotted lines) where applying P is indicated by red color and P^{-1} by blue color. For comparison the UDD values of δ_j $(j = 1, \ldots, n)$ are shown with gray lines in the respective linestyle. Note that for $n = 3$ UDD solution exists only for the single spin operations.

V. CONCLUSIONS

In this paper, we have considered exchange-only based echo sequences for three electron spins. We have shown that, in addition to the UDD-like optimized sequences introduced by West and Fong [6], the concept of OFDD can be applied to this three-spin case as well. We compared two different sequences of SWAP-based echo sequences, the one used in Ref. [6] and one which applies the same operation at every time $\delta_j T$. The optimal times according to UDD and OFDD depend on the choice of the sequence. The fidelity depends slightly on this choice with a small advantage for the all-cyclic permutation while the larger value of the minimum pulse interval can be an advantages of the West-Fong sequence in a realistic system. The improvement of the fidelity by the optimization strategies UDD and OFDD compared to the CPMG sequence is more significant for Ohmic noise than for Lorentzian noise. This could have been expected with respect to results for a single spin under the influence of high- and low-frequency noise [10].

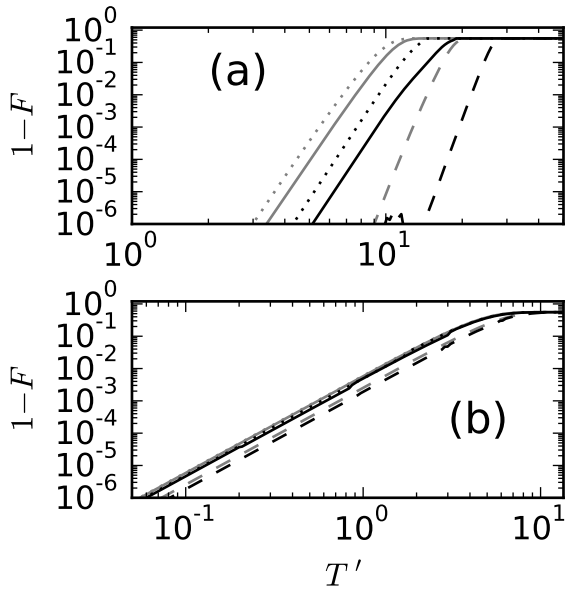

FIG. 7. (Color online) Comparison of UDD (gray) and OFDD (black) optimized values of infidelity $1-F$ in dependence of the dimensionless storage time T' for Ohmic (a) and Lorentzian (b) noise. For results are shown with dashed lines for single spin echos, with solid lines for the all-cyclic sequence, and with dotted lines for the West-Fong sequence. The number of pulses is $n = 10$.

ACKNOWLEDGMENTS

We thank Maximilian Russ for usefull discussions and the DFG for financial support under the programs SPP 1285 and SFB 767. GB acknowledges financial support from ARO through grant No. W911NF-15-1-0149.

APPENDIX A: FIDELITY OF A SPIN 1/2 IN A QUASI STATIC MAGNETIC FIELD

The fidelity of a quantum gate U acting on a single qubit in comparison to a desired gate U_0 is given by [15]

$$F = \frac{2 + |\operatorname{Tr}(U_0 U^\dagger)|^2}{6}. \tag{A1}$$

Here we define U_0 as the single-qubit rotation around the z axis about the angle $B_{\text{ext}}t$, i.e. the time evolution operator at time t for $\mathbf{B}^O = 0$. The operator U is the time evolution under the Hamiltonian $H = (B_{\text{ext}}\mathbf{e}_z + \mathbf{B}^O)\cdot\boldsymbol{\sigma}$ with an unknown, in general non-zero Overhauser field $\mathbf{B}^O$. We find at time t

$$\begin{aligned}\operatorname{Tr}(U_0U^\dagger) &= 2\cos((\omega - B_{\text{ext}})t)\\ &- (\cos((\omega-B_{\text{ext}})t) - \cos((\omega+B_{\text{ext}})t))(1 - \tfrac{B_{\text{ext}}+B_z^O}{\omega})\end{aligned} \tag{A2}$$

with $\omega = \sqrt{(B_{\text{ext}}+B_z^O)^2 + (B_x^O)^2 + (B_y^O)^2}$. For $B_{\text{ext}} \gg |\mathbf{B}^O|$ in lowest order,

$$1 - \frac{B_{\text{ext}}+B_z^O}{\omega} \approx \frac{(B_x^O)^2 + (B_y^O)^2}{(B^{\text{ext}})^2} \tag{A3}$$

which is negligible. Therefore the respective term in Eq. (A2) is small and can be neglected for all times t. The fidelity F is therefore approximated by

$$F \approx \frac{2 + 4\cos^2(B_z^O t)}{6} \tag{A4}$$

for times $t \lesssim 2\pi/(\omega - B_{\text{ext}})$ where we expanded ω in linear order in $\mathbf{B}^O$. This means that on relevant time scales, i.e. where the gate fidelity F is still close to one, the dephasing due to an Overhauser field is determined by the component parallel to the (strong) external magnetic field. Therefore, we have to deal only with commuting operators within the echo schemes discussed in this paper.

APPENDIX B: DETAILS ON THE FILTER FUNCTION AND THE FIDELITY CALCULATIONS

Here we give further details on our calculations. We present the filter functions for the three echo pulse sequences considered in this work. To avoid confusion we use the upper indices SO, WF, and AC for the sequence with single-spin operations, the sequence introduced by West and Fong [6], and the all cyclic sequence, respectively. We can always write

$$y_k(\omega T) = \sum_{j=0}^{n+1} \alpha_{kj} e^{i\omega T\delta_j} \tag{B1}$$

with $k = 1, 2, 3$ and α_{kj} being real. For the filter function we obtain

$$\begin{aligned}F_F(\omega T) &= \sum_{j,j'=0}^{n+1} \beta_{jj'} \cos(\omega T[\delta_j - \delta_{j'}])\\ &= \sum_{j,j'=0}^{n+1} \beta_{jj'}\{\cos(\omega T[\delta_j - \delta_{j'}]) - 1\}.\end{aligned} \tag{B2}$$

with $\beta_{jj'} = \sum_{k=1}^{3} \alpha_{kj}\alpha_{kj'}$. The second relation in Eq. (B2) holds because $|y_k(0)|^2 = \sum_{j,j'=1}^{n+1} \alpha_{kj}\alpha_{kj'} = 0$. For all sequences, $\alpha_{10} = -\alpha_{20} = 1$ and $\alpha_{3j} = -\alpha_{1j} - \alpha_{2j}$.

For the single-spin operations the coefficients α_{kj} are given by $\alpha_{1,n+1}^{\text{SO}} = (-1)^n$, $\alpha_{1j}^{\text{SO}} = 2(-1)^j$ $(1 \le j \le n)$, and $\alpha_{2j}^{\text{SO}} = -\alpha_{1j}^{\text{SO}}$. For the sequence introduced by West and Fong [6], the coefficients are

$$\{\alpha_{1,n+1}^{\text{WF}}, \alpha_{2,n+1}^{\text{WF}}\} = \begin{cases}\{-1, 1\} & \text{if } n \bmod 4 = 0,\\ \{1, 0\} & \text{if } n \bmod 4 = 1 \text{ or } 3,\\ \{0, -1\} & \text{if } n \bmod 4 = 2,\end{cases}$$

and for $j \in \{1, \ldots, n\}$

$$\{\alpha_{1j}^{\rm WF}, \alpha_{2j}^{\rm WF}\} = \begin{cases} \{-2,1\} & \text{if } j \bmod 4 = 1, \\ \{1,1\} & \text{if } j \bmod 4 = 2, \\ \{-1,-1\} & \text{if } j \bmod 4 = 3, \\ \{2,-1\} & \text{if } j \bmod 4 = 0. \end{cases}$$

The all P sequence has the coefficients

$$\{\alpha_{1,n+1}^{\rm AC}, \alpha_{2,n+1}^{\rm AC}\} = \begin{cases} \{1,-1\} & \text{if } n \bmod 3 = 0, \\ \{-1,0\} & \text{if } n \bmod 3 = 1, \\ \{0,1\} & \text{if } n \bmod 3 = 2, \end{cases}$$

and for $j \in \{1, \ldots, n\}$

$$\{\alpha_{1j}^{\rm AC}, \alpha_{2j}^{\rm AC}\} = \begin{cases} \{-2,1\} & \text{if } j \bmod 3 = 1, \\ \{1,1\} & \text{if } j \bmod 3 = 2, \\ \{1,-2\} & \text{if } j \bmod 3 = 0. \end{cases}$$

For OFDD we need to compute the integral $\int_0^1 d\omega'\, F_F(\omega' T')$ which can be easily done as

$$\int_0^1 d\omega'\, \cos(\omega' T' \Delta) = \frac{\sin(T'\Delta)}{T'\Delta}. \tag{B3}$$

To compute the integral in Eq. (15) we use for the Ohmic noise spectrum the integral

$$\int_0^1 d\omega'\, \frac{1-\cos(\omega' T' \Delta)}{\omega'} = \mathrm{Cin}(T'\Delta), \tag{B4}$$

where $\mathrm{Cin}(t) = \int_0^t dt'\, [1-\cos(t')]/t'$ is the cosine integral. For calculating the fidelity in the case of Lorentzian noise the following integral is used

$$\int_0^\infty d\omega'\, \frac{1-\cos(\omega' T' \Delta)}{\omega'^2(1+\omega'^2)} = \frac{\pi}{2}(e^{-T'\Delta} - 1 + T'\Delta). \tag{B5}$$

[1] D. P. DiVincenzo, D. Bacon, J. Kempe, G. Burkard, and K. B. Whaley, Nature (London) **408**, 339 (2000).
[2] J. Medford, J. Beil, J. M. Taylor, E. I. Rashba, H. Lu, A. C. Gossard, and C. M. Marcus, Phys. Rev. Lett. **111**, 050501 (2013).
[3] J. M. Taylor, V. Srinivasa, and J. Medford, Phys. Rev. Lett. **111**, 050502 (2013).
[4] J.-T. Hung, J. Fei, M. Friesen, and X. Hu, Phys. Rev. B **90**, 045308 (2014).
[5] In a strong external magnetic field only one leakage state need to be taken into account, see [4].
[6] J. R. West and B. H. Fong, New Journal of Physics **14**, 083002 (2012).
[7] G. T. Hickman, X. Wang, J. P. Kestner, and S. Das Sarma, Phys. Rev. B **88**, 161303 (2013).
[8] G. S. Uhrig, Phys. Rev. Lett. **98**, 100504 (2007).
[9] G. S. Uhrig, New Journal of Physics **10**, 083024 (2008).
[10] H. Uys, M. J. Biercuk, and J. J. Bollinger, Phys. Rev. Lett. **103**, 040501 (2009).
[11] D. Loss and D. P. DiVincenzo, Phys. Rev. A **57**, 120 (1998).
[12] J. R. Petta, A. C. Johnson, J. M. Taylor, E. A. Laird, A. Yacoby, M. D. Lukin, C. M. Marcus, M. P. Hanson, and A. C. Gossard, Science **309**, 2180 (2005).
[13] J. Taylor and M. Lukin, Quantum information processing **5**, 503 (2006).
[14] T. D. Ladd, Phys. Rev. B **86**, 125408 (2012)
[15] L. H. Pedersen, N. M. Møller, and K. Mølmer, Physics Letters A **367**, 47 (2007).
[16] G. de Lange, Z. H. Wang, D. Rist, V. V. Dobrovitski, and R. Hanson, Science **330**, 60 (2010).
[17] H. Y. Carr and E. M. Purcell, Phys. Rev. **94**, 630 (1954).
[18] S. Meiboom and D. Gill, Review of Scientific Instruments **29**, 688 (1958).
[19] J. R. West, B. H. Fong, and D. A. Lidar, Phys. Rev. Lett. **104**, 130501 (2010).
[20] G. S. Uhrig and D. A. Lidar, Phys. Rev. A **82**, 012301, (2010)